CHARACTERIZATION OF AISI 317L STEEL WELD CLADDING ON ASTM A516 GR 60 STEEL USED IN OIL AND GAS SECTOR

Marcos Mesquita da Silva, marcos_m_silva@yahoo.com.br
Danielton Gomes dos Santos, danielton_santos@yahoo.com.br
Marco Antonio dos Santos, santos@dem.ufcg.edu.br
Theophilo Moura Maciel, theo@dem.ufcg.edu.br
Federal University of Campina Grande, LABSOL/DEM/UFCG, Zip Code: 58429-900, Campina Grande – PB, Brazil

Marcelo Ferreira Motta, marcelo@ufc.br
Federal University of Ceará, ENGESOLDA/UFC, Zip Code: 60455-760, Fortaleza – CE, Brazil

Abstract. *The aim of this study was to characterize the metallurgical features and impact toughness of the interface between AISI 317L weld cladding and ASTM A516 Gr 60 steel. The weld cladding were carried out using the Twin Wire GMAW process and AWS E317L wire as filler with an interpass temperature of 423K. Two levels of heat input (H = 1170kJ/m and H = 1530kJ/m) and a mixture of argon and oxygen (95% Ar and 5% O_2) as shielding gas were used. The specimens were submitted to microtructure and microhardness analysis, and Charpy impact tests at room temperature and 273K. The results showed an increase in dilution and heat affect zone(HAZ) width when the heat input increased. Moreover, there was also the formation of hard zones (HZ) along the fusion line, presenting values above 300HV mainly for higher heat input levels.. The effect of heat input on Charpy energy specific values was more remarkable for the temperature of 273k and ranged from 1090 to 1480kJ/m^2.*

***Keywords**: Twin wire GMAW, Weld Cladding, AISI 317L, Hard Zones, Charpy impact test*

1. INTRODUCTION

Among the manufacturing and maintenance processes in oil and gas sector welding plays an important role. It is always present in all stages of these activities, and in many cases, it can become the critical process.

In this scenario two types of welding are very important, that is, similar and dissimilar welding. Similar welding refers to joining of alloy systems whose chemical compositions are roughly similar. During similar welding, the filler metal, when employed, also presents the same base metals characteristics, although it always possesses mechanical strength somewhat higher than these base metals. On the other hand, dissimilar welding refers to process of joining two alloy systems, when either the filler metal or one of the base metals is significantly different in chemical composition (Doody, 1992; Avery, 1991; Lippold and Kotecki, 2005).

In general, there are two welding dissimilar applications: transition joints and coatings (weld cladding) for protecting against corrosion. In the case of transition joints (or welded dissimilar metal joints), generally the base metals to be joined are ferritic and austenitic steels, and the filler metals employed are either austenitic stainless steels or nickel alloys. For economical reasons, this type of application has been utilized as transition joints in a variety of equipments. For instance, in the oil and gas industry the transition joints are sometimes used instead of flanged joints in wet and high temperature corrosive environments containing hydrogen sulfide and in high-pressure and temperature sour services (Omar, 1998; Doody, 1992). The same as transition joints, weld claddings – that are deposited by arc welding processes – are also quite common applications in the oil and gas industry, and the filler metals commonly used are also either austenitic stainless steels or nickel alloys. In the open literature it can be found several applications where austenitic stainless steels are deposited onto carbon steel substrates (Lundin, 1982; Hardie, 2004; Pashold *et al.*, 2007). The economic purposes for this application are the lower cost and higher mechanical strength of carbon steels (substrates) with regard to stainless steel (weld cladding). On the other hand, stainless steels have a good corrosion resistance that is required in applications where an aggressive fluid is in contact with some part of the equipment. Weld cladding can be applied to pressure vessels, piping and pipelines, storage tanks, oil distillation towers or any equipment (or component part) which require corrosion resistance (Lippold and Kotecki, 2005; Paranhos, 2008).

Nevertheless, during the deposit of weld cladding fabrication and metallurgical drawbacks can occur. One of metallurgical drawbacks during dissimilar welding between austenitic stainless steel and carbon steel is the dilution level resulted from the welding process and parameters. The lower the dilution the lower the likelihood of forming brittle microstructures susceptible to corrosion and/or the hydrogen embrittlement (Wainer *et al.*, 1992; Omar, 1998). On the other hand, due to differences between the chemical composition of austenitic stainless steel and carbon steel, and welding conditions, hard zone (HZ) – with hardness above 300HV – can form along the fusion line of the substrate side. These zones are very thin layers, up to 75μm, . with composition between the base metal (BM) and the bulk weld metal (WM) which can occur with several shapes and sizes. In the literature, these hard zones are also mentioned as partially diluted zones, transition zones, unmixed zones or intermediate mixed zones, which can consist of martensite, precipitates and/or intermetallic constituents such as *Sigma* e *Chi* phases (Doody, 1992; Wang, 1993; Omar, 1998; Kejelin *et al.*, 2005).

Due to the chemical composition gradient and, therefore, a microstructural gradient across the weld interface, there will be also a change in mechanical properties in this region. In general, such phenomena occur over a very short span. For instance, a change of 240HV – because of the formation of hard zones – may be approximately equivalent to a change of 689MPa in local strength (Lundin, 1982). Thus, there is still demand for researches about the characterization of mechanical properties across the weld interface. For this characterization several testing methods can be carried out, such as microhardness, tensile, impact and fracture toughness tests.

Because of the characteristics cited above, the hard zones become susceptible to localized pitting corrosion attack, hydrogen embrittlement and sulfide stress cracking, that can result in failures, during service, at weld interface of structure. The main types of failures observed at theses interfaces are cracking along the grain boundaries in the weld cladding deposit and cracking in regions with low mechanical strength due to carbon migration to weld metal (Omar, 1998; Rowe *et al.*, 1999; Lippold and Kotecki, 2005).

In view of the aforementioned, it becomes indispensable to find welding conditions that reduce or even eliminate these hard zones so that the chances of occurring failures are also reduced.

Thus, the aim of this study was to characterize the metallurgical features and impact toughness of interface between AISI 317L weld cladding and ASTM A516 Gr 60 steel.

2. MATERIALS AND EXPERIMENTAL PROCEDURE

2.1. Materials

The substrate used in this work was an ASTM A516 Gr 60 steel. It was received in form of 0.0125m-thick plate. This plate was cut into 0.064x0.160m coupons, as can be showed in Fig. 1 (a and b). The weld claddings were deposited into the central groove of coupons.

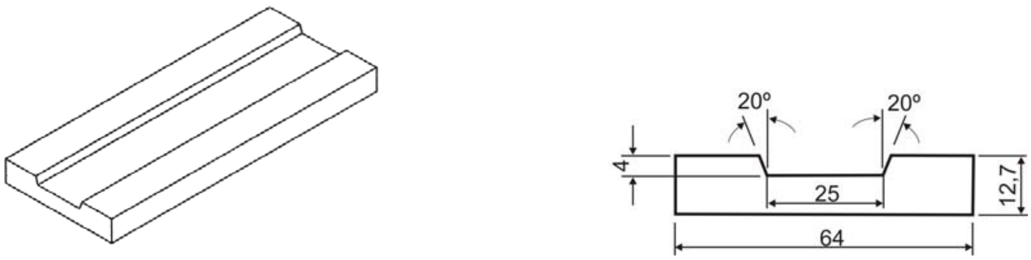

(a) (b)

Figure 1. Machined substrate coupon: (a) 3D-coupon; (b) cross section of coupon with its main dimensions (in mm).

The chemical compositions of the weld cladding and substrate are listed in Tabs. 1 and 2, respectively.

Table 1. Specification of chemical composition for ASTM A516 Gr 60 steel.

ASTM A516 Gr 60	Composition (wt-%)				
	C*	Mn	P*	S*	Si
	0.21	0.60- 0.90	0.035	0.035	0.15- 0.40

* Specified maximum. Font: ASTM, (2004).

Table 2. Nominal chemical composition of the metal filler AWS E317L.

Metal Filler	Composition (wt-%)						
	C	Cr	Ni	Mo	Fe	Mn	Si
E317L	0.03	18.50	13.00	3.80	8.00	1.00	0.70

Font: BÖHLER (2008).

2.2. Welding Procedures

The depositions of the AISI 317L weld claddings on ASTM A516 Gr 60 steel substrates were carried out by the Twin Wire GMAW process. Table 3 contains the main welding parameters employed during the wed cladding deposits, where I(A) is the welding current, S_W is the welding speed and H is the heat input. These weld cladding were carried out in the Laboratory of welding Engineering (ENGESOLDA) in the Federal University of Ceará. All the welding was executed with an interpass temperature of 423K (150ºC). The welds were executed by an industrial robot and, as shielding gas, it was used a mixture of 95% Ar and 5% O_2.

Table 3. Welding Parameters used.

Coupons	I (A)	S_W (m/s)	H (kJ/m)
1	170	$6.7\text{x}10^{-3}$	1530
2	130	$6.7\text{x}10^{-3}$	1170
3	170	$8.7\text{x}10^{-3}$	1170
4	170	$6.7\text{x}10^{-3}$	1530

2.3. Metallographic Procedures

After welding the samples were transversally cut for metallographic analysis. These analysis were executed in the Metallography Laboratory of Mechanical Engineering Department of the Federal University of Campina Grande (DEM/UFCG). Conventional techniques, of cutting, mounting, grinding, polishing, were done and nital (1,5%) was used as etchant.

The dilutions were calculated for each welding condition, using the Eq. (1). The areas 1 and 2 (Fig. 2) were calculated using a CAD program.

$$Diluition\ (\%) = \left(\frac{area\ 2}{area\ 1 + area\ 2}\right) \times 100\% \qquad (1)$$

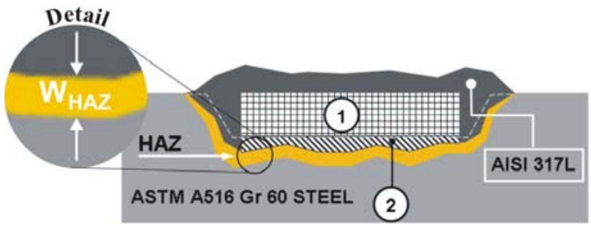

Figure 2. Identification of the areas for dilutions calculation.

The lateral dilutions of groove did not participate in the Eq. (1) because it should not be the best way to simulate a real weld cladding application. On the other hand, the width of HAZ (W_{HAZ}) was measured according to the detail in Fig. 2. A mean W_{HAZ} was obtained as a result of three measurements taken along the section

2.4. Microhardness Surveys

The microhardness tests were conducted using two methodologies. In the first the indentations were made along six vertical lines (Fig. 3a), being used a load of 0.3kg and loading time of 15 seconds. This method was adopted in order to observe the hardness gradient along the WM, HAZ and BM. The distance between indentations in the WM was 500µm (0.5mm), whereas in HAZ and BM this distance was 250µm (0.25mm). In the second methodology the indentations were executed adjacent to fusion line, inside the AISI 317L WM (Fig. 3b). For this, a load of 0.1kg was applied for 15s for each indentation. The load was reduced from 0.3 to 0.1kg in order avoid the indentation sizes be not larger than the HZ width. In this second method, the distance between indentations was 250µm (0.25mm).

(a) (b)

Figure 3. Methodologies for microhardness testing: (a) indentations along the vertical lines (and load of 0.3kg) and (b) indentations along the fusion boundary, inside the WM (load of 0.1kg).

2.5. Charpy Impact Testing

Charpy V-notch (CVN) subspecimens were machined from the welded coupons. Figure 4 shows the orientation of the sample in the welded coupon. Charpy impact testing was done at 273 and 298K test temperatures. Sub specimens of 5x10x55(10^{-3}m) were machined in order to be possible localize the V-notch tip at boundary fusion (Fig. 4). Charpy Impact testing was done as ASTM E 23-02a standard.

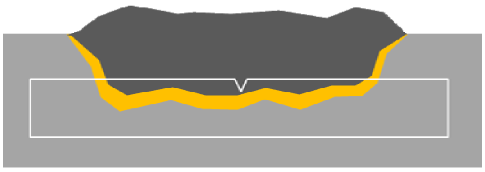

Figure 4. Localization of the CNV subspecimen in welded coupon.

3. Results and Discussion

3.1. Metallographic Examination

Figure 5a presents the cross section macrograph of welded coupon, indicating the HAZ width. It was verified that for an increase of 360 kJ/m in the average heat input, the average HAZ width has increased by 5x10^{-4} m as can showed in figure 5 (b)..

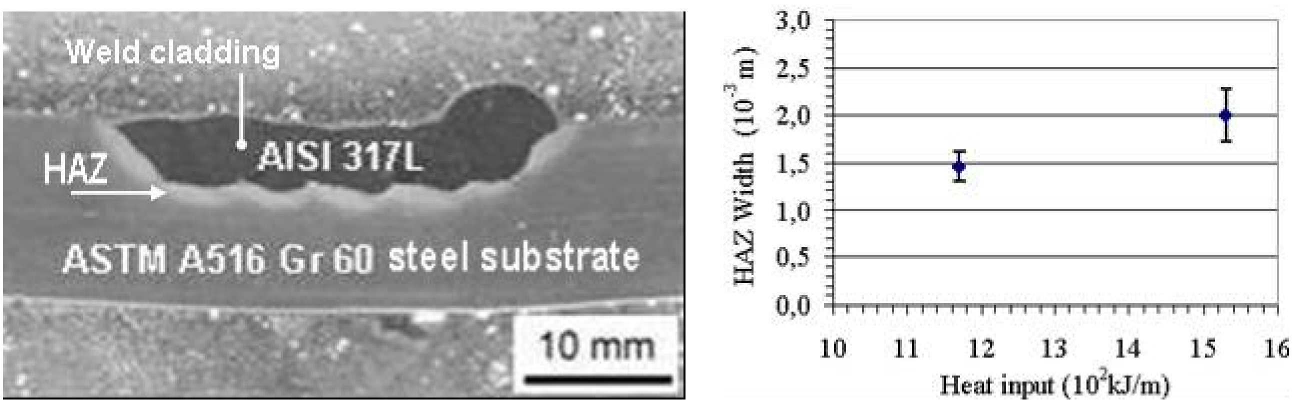

(a) (b)

Figure 5. (a) Macrograph of cross section of welded coupon (etchant: nital 1.5%), (b) effect of heat input on the HAZ width.

Figure 6a shows the influence of heat input (H) on dilution. In Figure 6b, it can be observed the effects of welding current and speed on the dilution. Table 4 summarizes the influences of all welding parameters on dilution.

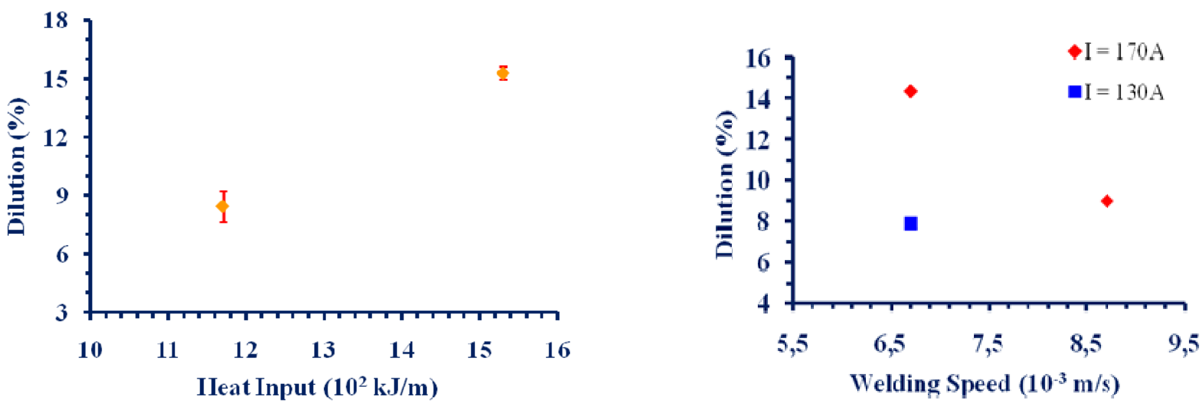

(a) (b)

Figure 6. (a) Influence of heat input and (b) welding current and speed on dilution.

Table 4. Effect of welding parameters on dilution.

Coupons	I (A)	S_W (m/s)	H (kJ/m)	Dilution (%)
1	170	$6.7x10^{-3}$	1530	13.88
2	130	$6.7x10^{-3}$	1170	7.90
3	170	$8.7x10^{-3}$	1170	9.02
4	170	$6.7x10^{-3}$	1530	14.35

From Figure 6a and Tab. 4, it can be noted that for an increase of 360 kJ/m in the average heat input, there was an increase of 5.6% in the average dilution level. So, it can be observed that lower dilution values were obtained for lower values of heat input and welding current, and higher welding speeds. It can be also verified, from Fig. 6b, that is possible to obtain dilution values roughly equivalent for different current values since that the welding speed (S_W) values are changed. For the welding parameters used in this work, the lowest dilution value was of 7.90% whereas the highest one was of 14.35% (Tab. 4). The higher the dilution, the greater the participation of iron and carbon in the weld metal. Thus, a low dilution is always desired in order to reduce the formation hard and brittle microstructures and susceptible to corrosion attack. Furthermore, low dilution also aids avoiding weld solidification cracking (Lippold and Kotecki, 2005; Kejelin *et al.*, 2005). Rowe *et al.* (1999) reached an improvement in the stainless steel weld cladding strength to the cracking near the weld interface when they reduced the dilution level from 40 to 30% for ER308 filler metal.

In regard to the weld interface, some metallurgical features were observed. For both heat input levels (H=1170kJ/m and H=1530kJ/m) occurred formation of peculiar regions with differing shape, size and appearances, as can be seen in Figs. 7 and 8, although for H=1530kJ/m these regions occurred with more frequency. Figure 7a, presents a narrow band ("beach") into the weld metal (WM) along the fusion boundary (FB), with high microhardness values (hard zones-HZ). Fig. 7b presents another HZ with different morphology ("peninsula"), which corresponds to an area partially enclosed by carbon steel base metal.

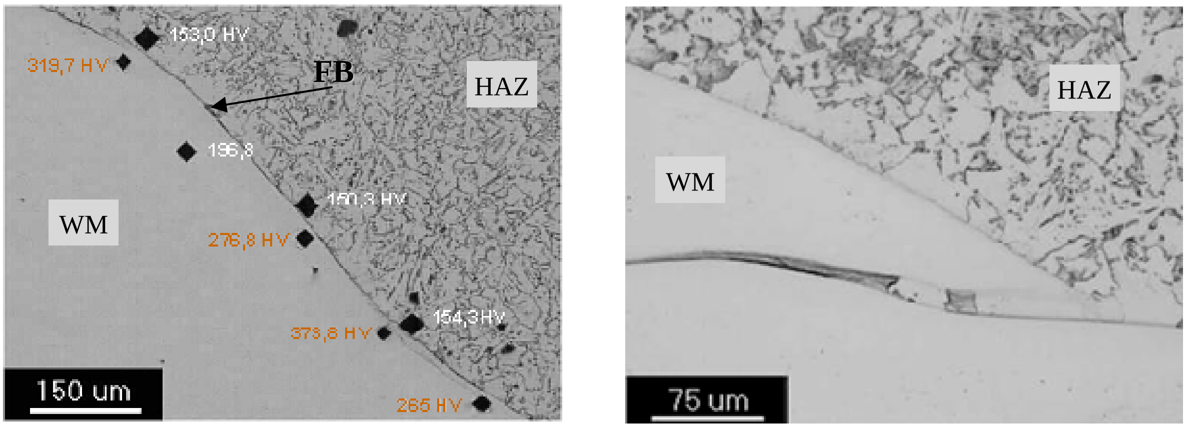

(a) (b)

Figure 7. Morphologies of regions that contain HZ: (a) "Beach" and (b) "Peninsula". Etchant: Nital 1.5% (for 15s).

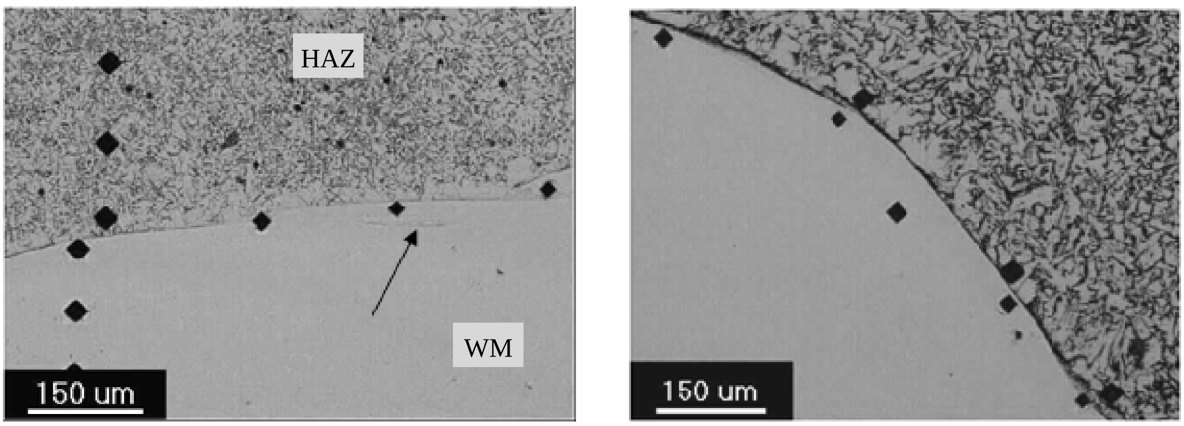

(a) (b)

Figure 8. (a) Small "Island" (1.5% nital etchant, for 15s). (b) "Beach" (1.5% nital etchant, for 180s).

Another type of these regions is completely enclosed by carbon steel base metal ("island"). Figure 8a, shows small "island" similar to that found by Doody (1992). All this kind of regions deserves special attention because in their boundaries generally there are hard zones presenting hardness above 300HV.

The "beach" in Fig. 7a is the same region in Fig. 8b, but the later was etched with 1.5% nital for 180s, and as can be verified in Fig. 8b, the microstructure of this region was not sensitive to this etching type. Nevertheless, it is noted in Fig. 9a that there were evident HZ which were etched by the same way. Figure 9b presents the same HZ of Fig. 9a. It can be observed an acicular structure similar to martensite. The width of this hard zone was up to 48μm (Fig. 9b). In the literature can be found hard zone widths from 10 to 75μm (Doody, 1992; Kou and Yang, 2007). HZ may also contain precipitates or intermetallic formed during welding (Lundin, 1982; Omar 1998). Thus it is important to use other chemicals reagents for etching and analyzing that HZ it in more details.

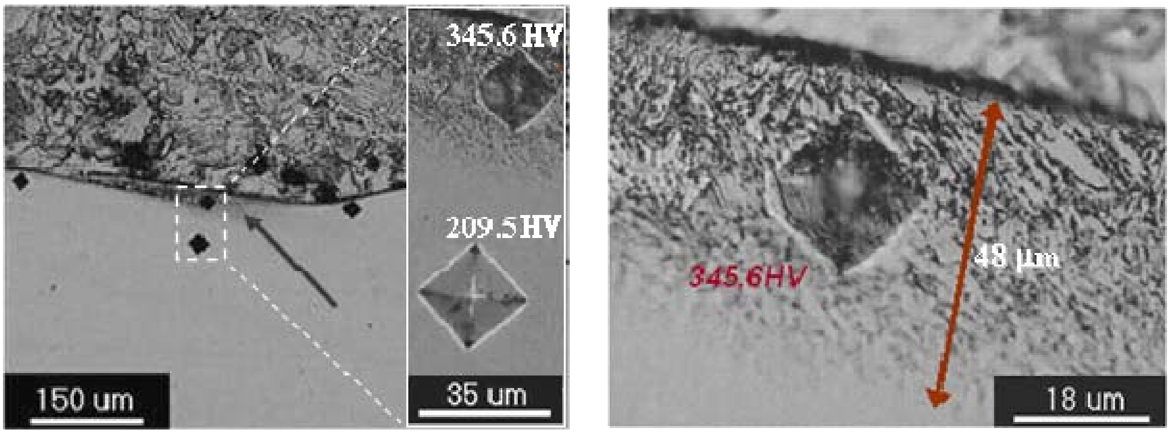

Figure 9. (a) Hard zone microstructure (100X and 500X). (b) The same microstructure (1000x). Etchant: 1.5% nital (for 180s).

3.2. Microhardness

The hardness gradients along the regions WM, HAZ and BM, can be verified in Figs. 10a and 10b, for H=1530kJ/m and H=1170kJ/m, respectively. It is verified, for both heat input levels, that the WM presents a higher hardness level than the HAZ, and the HAZ hardness is slightly higher than the BM. It is also observed that there were not significant variations in the hardness gradients for the two heat input levels. In terms of average values, for H = 1530 kJ/m, the hardness of the bulk WM and HAZ were 180.0HV ± 9.0 HV and 152.0 ± 6.0 HV, respectively. And for H = 1170kJ/m, the hardness of the bulk WM and HAZ were 182.0HV ± 8.0 HV and 158.0 ± 7.0 HV, respectively. The BM presented a average hardness of 145.0 ± 4.0 HV.

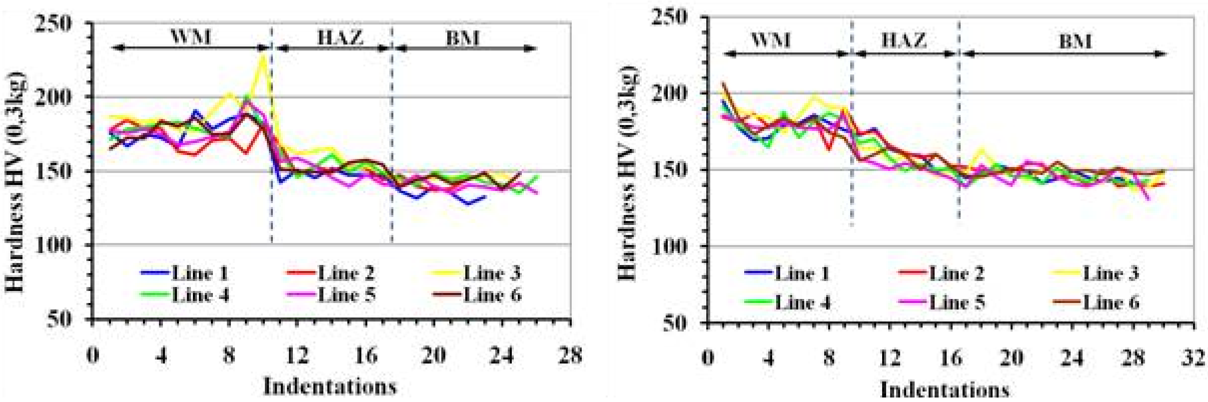

Figure 10. Microhardness along the vertical lines for (a) H = 1530 kJ/m and (b) H = 1170 kJ/m.

Although it is not a significant variation, the HAZ hardness values for H=1170kJ/m was slightly higher than that for H=1530kJ/m. This difference was of 6HV, in terms of average value. The lower heat input weld passes undoubtedly result in higher cooling rates. (Barnhouse and Lippold, 1998; Kejelin *et al.*, 2008). But, it should be remembered that base metal thickness also influences on cooling rates. Kejelin *et al.* (2008) obtained, for a 1.15%Mn–steel, an increase in the coarse grain HAZ hardness of 20HV when they increased the heat input by 400kJ/m. However, the pipe thickness was 0.02m. In the current study the base metal thickness was 0.0127m, and after 0.004m-depth groove machining the new thickness of plate became 0.0087m (Fig. 1b). This fact can explain the small variation in cooling rates and, therefore, in HAZ hardness levels.

The hardness of the regions adjacent to the fusion boundary was measured in according to the methodology from Fig. 3b. Figures 11a and 11b present in graphic form the hardness values at the fusion boundary for both heat input levels. It is noted that for H=1530kJ/m (Fig. 11a) occurred more values above 250HV. This value of 250HV is a limit required by NACE (National Association of Corrosion Engineers) for the maximum hardness of carbon and stainless steel base metals and weld deposits in wet sour services (Doody, 1992; Omar, 1998). Although NACE does not address the hardness of HZ from dissimilar welding, this limit can be used for comparative effect.

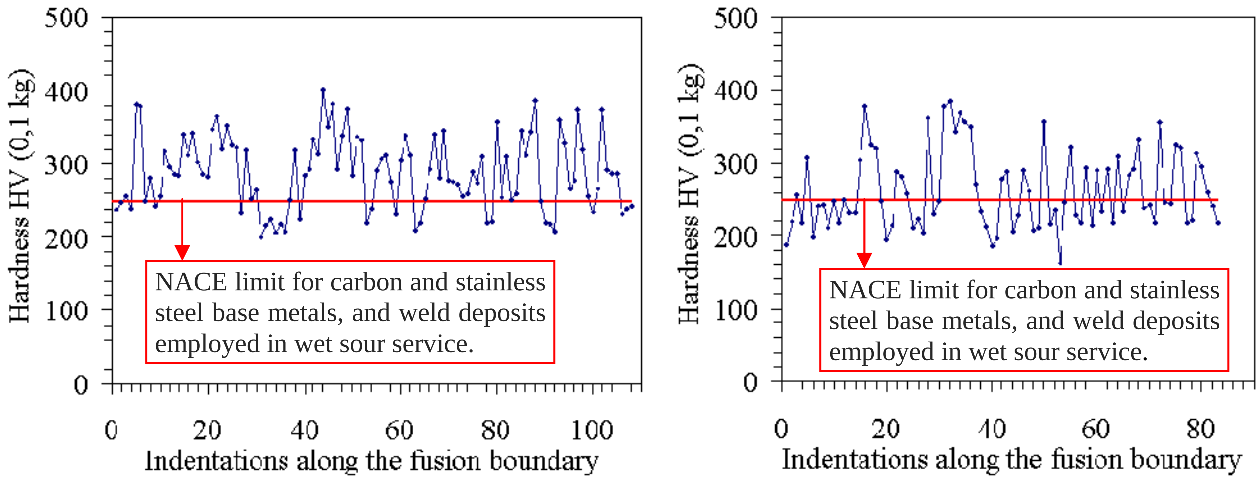

(a) (b)

Figure 11. Gradient of the hardness along the fusion boundary: (a) for H = 1530 kJ/m and (b) H = 1170kJ/m.

Table 5 shows a comparative and quantitative form of the microhardness test results along the fusion boundary for both heat input levels. From Table 5 it is observed that 74.07% of the indentations presented hardness values above the limit established by NACE, for H=1530 kJ/m, whereas for H=1170kJ/m this percentage was of 32.53%. This same analysis, in Tab. 5, can be done for other hardness levels such as 300, 350 and 400HV. So, there was a reduction in hardness when H was reduced by 360kJ/m. These results are consistent with those obtained for dilution (Fig. 6a and Tab. 4), since the heat input of 1170kJ/m provided lower dilution values and, consequently, reducing the amount of brittle and hard microstructures.

Table 5. Comparison between the hardness levels along the FB for H=1530 kJ/m and H=1170 kJ/m.

Indentations along the fusion boundary (FB)				
Hardness level	H = 1530 kJ/m		H = 1170 kJ/m	
	Number of indentations	Percents	Number of indentations	Percents
Hardness above 200HV	107	99.07%	77	92.77%
Hardness above 250HV*	80	74.07%	27	32.53%
Hardness above 300HV	43	39.81%	20	24.10%
Hardness above 350HV	13	12.04%	8	9.64%
Hardness above 400HV	1	0.93%	0	0.00%
Total of indentations	108		83	

* NACE limit.

Indentations whose hardness values are above 300HV indicates a presence of HZ at the weld interface (FB). This fact was confirmed by metallographic examination (Figs. 7, 8 and 9). From Table 5 it can be seen that the amount of indentations – whose hardness values were above for H=1170kJ/m – was reduced by 15.71% when compared with those for H=1530kJ/m. Kejelin *et al.* (2008) found that amount of HZ was diminished when heat input was also diminished, although no quantitative method had been shown.

These HZ are undesirable metallurgical phenomenons during a dissimilar welding, because they are areas susceptible to the located pitting corrosion attack, hydrogen embrittlement and sulfide stress cracking, that can result in failures, during service, at weld interface of structure (Omar, 1998; Rowe *et al.*, 1999; Lippold and Kotecki, 2005). According to literature, the high hardness levels can be eliminated only by the elimination of HZ. The most important factors which promote formation of HZ are the filler and base metal chemical compositions plus the cooling rate during welding (Omar, 1998). Besides the heat input, the cooling rate is influenced by preheating temperature and thickness of the substrate. In regard to post welding heat treatment (PWHT), it seems be unanimous among researchers that it presents a negative effect on mechanical properties of the structure containing HZ. The main causes for this negative effect are: the carbon migration from BM to WM and the consequent loss of mechanical strength of the carbon-poor region (Lundin, 1982; Omar, 1998; Lippold and Kotecki, 2005). Thus, in future studies other welding parameters, mainly preheating, will be altered in order to minimize still more or until eliminating the occurrence of these HZ.

3.3. Chary Impact Toughness

Figures 11a and 11b show the effect of heat input on specific Charpy energy (SCE) values at the temperatures of 273 and 298K. In this work specific Charpy energy (SCE) is defined as the Charpy energy obtained from the tests divided by fracture area of subspecimen. Figure 12a shows the effect of the heat input on the specific Charpy energy for T=298K. Taking into account the standard deviations verified for the SCE, it can be noted that there was no significant influence of heat input on SCE at the temperature of 298K. On the other hand, in Fig. 12b it is observed that the effect of the heat input on the SCE values was more remarkable, at T=273K. For an increase of 360kJ/m in the heat input the average SCE increased by 390kJ/m^2. Table 6 summarizes all the Charpy impact test results. From this table it can be seen that the higher SCE value was 1690kJ/m^2 (1480 + 210kJ/m^2) at T=273K. Taban *et al.* (2008) obtained a SCE value of 1725kJ/m^2, using a standard Charpy specimen with notch localized at weld interface, for a 1.53%Mn-steel at T=273K. This value of 1725kJ/m^2 is close to that (1690kJ/m^2), although in the current work Charpy subspecimens have been used.

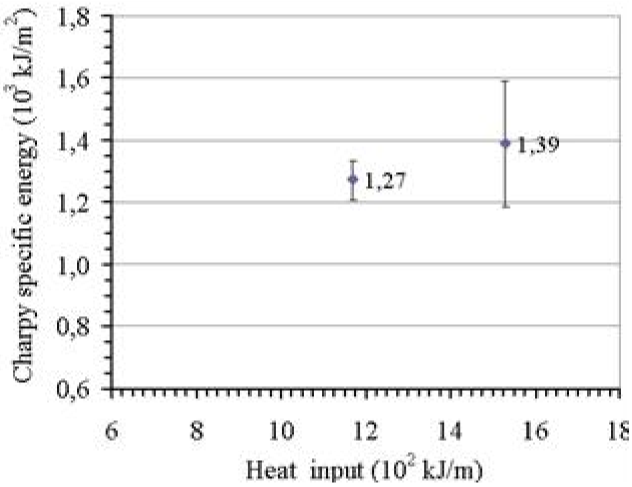

(a)

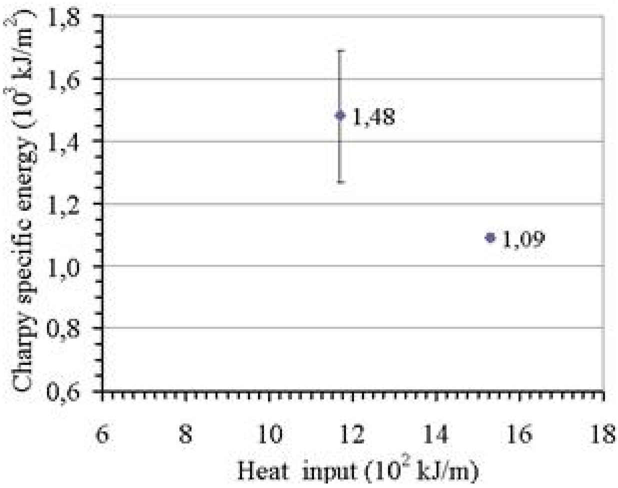

(b)

Figure 12. Effect of heat input on Charpy specific energy at: (a) T = 298K and (b) T = 273K.

Table 6. Influence of heat input on SCE values.

Temperature	H=1170kJ/m		H=1530kJ/m	
	average SCE values	Standard deviation	average SCE values	Standard deviation
T=298K	1270kJ/m^2	± 60 kJ/m^2	± 1390kJ/m^2	± 202 kJ/m^2
T=273K	1480kJ/m^2	± 210 kJ/m^2	± 1090kJ/m^2	± 10 kJ/m^2

In spite of weld interface has presented HZ, the results from Charpy impact tests does not seem to be enough to characterize negative effect of low impact resistance, probably because it were small in bulk specimen. Pope *et al.* (2004) mentioned that there must be at least 10% of HZ on the path of fracture cracking for the effect of these zones to be noticed. In future studies CTOD fracture toughness testing will be led in order to characterize the effects of these HZ on fracture toughness of the weld interface.

Nevertheless, the SCE results can be correlated with those of HAZ width. It was noted that for an increase of 5x10^{-3}m in the average HAZ width occurred a loss of 390kJ/m^2 in specific Charpy impact toughness value at 273K. In general, higher HAZ widths are associated with higher coarse grains, and this later associated with lower impact toughness (Barnhouse and Lippold, 1998; Taban *et al.* 2008).

4. Conclusion

- It was found that the HAZ width and dilution decreased when the heat input was reduced. For a reduction of 360kJ/m in heat input, there were reductions of $5x10^{-4}$m in HAZ width and 5.6% in dilution.
- For both heat input levels it was verified HZ located adjacent to fusion boundary with hardness values above 300HV. Several HZ presented acicular microstructure similar to martensite.
- A reduction of 360kJ/m in heat input implicated only in a slight increase of 6HV in HAZ hardness.
- The influence the heat input on specific Charpy energy was more remarkable at 273K. An increment of $5x10^{-4}$m in HAZ width implicated in a decrease in SCE of $0.39kJ/m^2$.

5. ACKNOWLEDGEMENTS

The authors thank to Conselho Nacional de Desenvolvimento Científico e Tecnológico (CNPq) and Finep (Financiadora de Estudos e Projetos) for sponsoring the research during the course of these investigations. The authors are also grateful to Agência Nacional de Petróleo, Gás e Biocombustíveis (ANP) through Programa de Recursos Humanos (PRH-25) of the Federal University of Campina Grande (UFCG) for the support to research and logistic facilities.

6. REFERENCES

AMERICAN SOCIETY FOR TESTING AND MATERIALS (ASTM), 2004, A516/516M: Standard Specification for Pressure Vessel Plates, Carbon Steel, for Moderate – and Lower-Temperature Service. United States.

Avery, Richard E., 1991, "Pay attention to dissimilar-metal welds", Chemical Engineering Progress, Vol. 87, No. 5, pp.70-75.

BÖHLER WELDING GROUP. Aceros Inoxidables. 27 October 2008, <http://www.bohlerweldinggroup.com.ar/spanish/50_ESN_HTML.htm>.

Barnhouse, E. J.; Lippold, J. C., 1998, "Microstructure/Property Relationship in Dissimilar Welds Between Duplex Stainless Steels and Carbon Steels", Welding Journal, Vol. 77, No. 12, pp. 477-487.

Doody, T., 1992, "Intermediate Mixed Zones in Dissimilar Metal Welds for Sour Service", Welding Journal**,** Vol. 71, No. 3, pp. 55-60.

Hardie, D. *et al*., 2004, "Hydrogen embrittlement of stainless steel overlay materials for hydrogenators", Corrosion Science, Vol. 46, pp.3089-3100.

Kejelin, Norton Z.; Buschinelli, Augusto J. A.; Pope, A. M., 2005, "Effect of Welding Parameters on the Partially Diluted Zones Formation at Dissimilar Metal Welds", Proceedings of the 18th Brazilian Congress of Mechanical Engineering, Vol.1, Ouro Preto, Brazil, pp. 1-8.

Kejelin, N. Z.; Buschinelli, A. J. A.; Bohórquez, C. E. N., "Soldagem Dissimilar do Aço X-60 com Inconel 625". 02 February 2008, <http://www.labsolda.ufsc.br/noticias/2007/soldagem_dissimilar.pdf>. Accessed on:.

Kou, S. and Yang, Y. K., 2007, " Fusion-Boundary Macrosegregatio in Dissimilar-Filler Wels", Welding Journal, Vol. 86, No. 10, pp. 303-312.

Lippold, J. C., and Kotecki, D. J., 2005, "Welding Metallurgy and Weldability of Stainless Steel. New Jersey: John Wiley & Sons, 357p.

Lundin, C. D., 1982, "Dissimilar Metal Welds: Transition Joints Literature Review", Welding Journal, Vol. 61, No. 2, pp.58-63.

Omar, A. A., 1998, "Effects of Welding Parameters on Hard Zones Formation at Dissimilar Metal Welds", Welding Journal, Vol. 77, No. 2, pp.86-93.

Paranhos, R.. "Revestimento de Aço Carbono com Aço Inoxidável Austenítico". 26 May 2008, <http://www.infosolda.com.br/download/12ddc.pdf>.

Paschold, R.; Karlsson, L., and Gittos, M. F., 2007, "Disbonding of Austenitic Weld Overlays in Hydroprocessing Applications", Svetsaren: The ESAB Welding and Cutting Journal, Vol. 62, No. 1, pp.10-15.

Pope, A. M.; Cardoso, A.; Chiapin, C. E. L.; Nascimento, J. L.; Teixeira, J. C. G.; Cunha, L. D. S., Paes, M. T. P., 2004, "Tenacidade à Fratura de Juntas Soldadas de Aços Dissimilares", 2nd ENSOLD-Encontro Técnico de Soldagem, Rio de Janeiro, Brazil.

Rowe, D.; Nelson, T. W.; Lippold, J. C., 1999, "Hydrogen-Induced Cracking Along the Fusion Boundary of Dissimilar Welds", Welding Journal, Vol. 78, No. 2, pp.31-37.

Taban, E.; Deleu, A.; Dhooge, A.; Kaluc, E., 2008, "Evaluation of Dissimilar Welds between Ferritic Stainless Steel Modified 12% Cr and Carbon Steel S335", Welding Journal, Vol. 87, No. 12, pp. 291-297.

Wainer, E.; Brandi, S. D.; Mello, F. D. H., 1992, "SOLDAGEM: Processos e Metalurgia", São Paulo: Edgard Blücher Ltda, 494p.

Wang, Zhihui; Xu, Biyu; Ye, Ciqi, 1993, "Study of the Martensite Structure at the Weld Interface and the Fracture Toughness of Dissimilar Metals Joints", Welding Journal, Vol. 72, No. 8, pp.397-402.

7. RESPONSIBILITY NOTICE

The author(s) is (are) the only responsible for the printed material included in this paper.